

The measurement of echo direction in a phased-array radar

F.B. Rijdsijk\* and

Key words:

G.A. van der Spek

radar

Physics Laboratory TNO

arrays

The Hague, The Netherlands

monopulse

Summary

For a planar-array antenna with a monopulse feed horn a simple algorithm for the determination of the direction of target echoes is described. Antenna pattern measurements of the array indicate that the direction sines of a received wavefront can be independently obtained with one simple relation between a normalized difference channel output and a direction sine.

The accuracy of the algorithm is determined.

---

\*presently with N.V. Philips Gloeilampen Fabrieken, department for Scientific and Industrial Equipment, Eindhoven, The Netherlands.

## 1.0 Introduction

One of the basic tasks of many radar systems is to estimate the direction of detected targets. In a phased-array radar system the obvious way to obtain target direction is by applying some form of monopulse [1]. In this paper a monopulse system is considered which operates with two difference channels and one sum channel.

When, during search, a target is illuminated by the radar's transmission beam, echo signals can be obtained via the two difference beams and an additional sum reception beam (which is identical to the antenna's transmission beam).

The magnitude and phase of the two difference channel outputs relative to those of the sum channel output convey all the relevant information about the direction of the echo. The nature and degree of complication of the relations between the actual angular target position and the magnitudes and phases of the signals received via the three reception channels determine the feasibility of the monopulse process.

The dependence on the scanning direction should be simple. The resulting estimation accuracy should be sufficient.

The purpose of this paper is to demonstrate this feasibility by measurements done with an actual phased-array antenna.

## 2. Phased-array antenna

The phased-array antenna (CAISSA) used for this investigation has been designed and built by the Physics Laboratory of the Netherlands Organization for Applied Scientific Research TNO in co-operation with Hollandse Signaal-apparaten. The latter did part of the production of the phase-shifters and constructed the monopulse feed horn.

It is a space-fed lens-type planar circular array with 847 active and 325 dummy elements, illuminated by a horn. The non-reciprocal ferrite phase-shift elements have a 4 bits phase setting. The 3-dB beamwidth of the pencil beam in broadside is approximately 4 degrees. The multi-mode feed horn provides one sum channel, used for transmission and reception, and two orthogonal difference channels for reception.

The antenna covers a frequency band from 5400-5900 MHz and has a useful scan angle of 60 degrees. The directivity in broadside is 33dB, the highest sidelobes are smaller than 5dB.

## 3. Beamforming [2]

When a target is to be illuminated the individual phase-shifters in the array are set such that the almost spherical waves arriving from the horn during transmission are transformed into plane waves directed towards the target (fig. 1a). This is realised by a phase correction over the aperture, consisting of a fixed part (near-spherical to planar) and a target direction dependent part. In fig. 1 the wavefronts are shown in a horizontal section through broadside parallel to the H-component of the linearly polarized field. On reception the reverse process takes place.

If target direction and transmission beam direction are not identical, the converging spherical waves will deviate from the horn axis. The relative magnitude and phase of the received signals in difference channel and sum channel determine the difference between supposed and actual target direc-

tion. In fig. 1 this is shown for one angular dimension. If the actual target direction is varied around the supposed target direction within the main beam the magnitude of the sum channel output ( $\Sigma$ ) will vary slightly around a maximum value, while that of the difference channel ( $\Delta H$ ) will vary considerably. The magnitude of the difference channel will be zero if the supposed and actual target directions coincide. The phase of the difference signal relative to that of the sum channel changes by  $180^\circ$  when the actual target direction moves over the supposed direction. The same applies to the other difference channel ( $\Delta E$  channel) in the plane perpendicular to that of fig. 1.

The sum- and difference antenna patterns are mainly determined by the illumination of the array by the horn. The desired illumination of the array for the difference channels (on reception only) is symmetrical in magnitude, with no illumination on the symmetry axes separating left and right part for the  $\Delta H$  channel and upper and lower part for the  $\Delta E$  channel.

The corresponding array halves have opposite phases after the correction from near-spherical to planar. The horn was designed such that the maxima of its difference patterns are close to the 3dB contour of its sum pattern.

Since the design goals have only been realized up to a certain degree and the radiation patterns of the horn had only been measured in the E and H planes, there was not enough information available to compute the sum and difference patterns of the complete antenna. Moreover the effect of the array lens can only be approximated in such a computation. Therefore it was decided to measure a set of sum and difference patterns of the antenna directly. With these measurements the performance of any angle measurement procedure can be determined.

#### 4. Angle estimation procedure

The direction of a target is obtained by estimating the difference in direction (two dimensions) between the direction in which a sum beam is radiated

$(u,v)$  and the actual target direction  $(u_t, v_t)$ .

This difference in direction is obtained by computing the quotients of the echo magnitudes in each difference channel and the sum channel, i.e.  $\frac{\Delta H}{\Sigma}$  and  $\frac{\Delta E}{\Sigma}$  and processing on them according to:

$$\left. \begin{aligned} \delta u &= f_{u,v,\text{freq}}^u \left( \frac{\Delta H}{\Sigma}, \frac{\Delta E}{\Sigma} \right) \\ \delta v &= g_{u,v,\text{freq}}^v \left( \frac{\Delta H}{\Sigma}, \frac{\Delta E}{\Sigma} \right) \end{aligned} \right\} (1)$$

so that the estimated target direction is given by

$$\left. \begin{aligned} \hat{u}_t &= u + \delta u \\ \hat{v}_t &= v + \delta v \end{aligned} \right\} (2)$$

The sign of  $\delta u$  (and  $\delta v$ ) is positive if  $\Sigma$  and  $\Delta H$  (and  $\Delta E$ ) have the same phase. This approach is similar to that discussed by Brennan [4], where squinted beams without normalization by a sum channel output are used.

The functions  $f_{u,v,\text{freq}}^u$  and  $g_{u,v,\text{freq}}^v$  depend on the choice of the angular co-ordinates and on the illumination of the array by the horn. By using phased-array co-ordinates (see para 5) the dependence on the scan direction  $(u, v)$  should vanish.

The applied illumination is such that it was expected that the following simpler relations might be obtained:

$$\left. \begin{aligned} \delta u &= f \left( \frac{\Delta H}{\Sigma} \right) \\ \delta v &= f \left( \frac{\Delta E}{\Sigma} \right) \end{aligned} \right\} (3)$$

These relations give rise to a much simpler angle estimation algorithm than those of (1):

- 1- the estimation is independent for both dimensions
- 2- the same processing is used for both dimensions
- 3- the processing is independent of scan direction
- 4- the processing is independent of frequency

From the measurements it will be shown that indeed the simpler relations are valid with sufficient accuracy.

#### 5. Phased-array co-ordinate system [3,2]

The appropriate co-ordinate system to be used is the phased-array co-ordinate system or sine space, in which the direction is characterized by two direction sines. In this system antenna patterns are independent of the scan direction.

The co-ordinates are  $R$ , the distance from antenna to target, and  $u = \sin A$  and  $v = \sin B$ . Any direction of observation can be characterized by the angles  $A$  and  $B$  or by  $\sin A$  and  $\sin B$ , where  $A$  and  $B$  are the angles between the line antenna-target and its projections on the  $YZ$ - and  $XZ$ -planes (see fig.2).

The antenna is placed in the  $XY$ -plane with its centre in the point  $(0,0,0)$  ( $XYZ$  is a rectangular Cartesian co-ordinate system).

When a sphere with unit radius is constructed, centred at the origin, the line from antenna centre towards the target intersects this sphere in  $P$ , with co-ordinates  $x = \sin A$ ,  $y = \sin B$ ,  $z = \sqrt{1 - \sin^2 A - \sin^2 B}$ .

By varying the angle  $A$  for constant values of  $B$   $P$  describes circles of constant  $\sin B$ . In a similar way circles of constant  $\sin A$  are obtained. The circles of one type do not intersect all circles of the other type and, if they do, the angle of intersection can have any value. Thus the phased-array co-ordinate system is not orthogonal. The angle  $\mu$  between two intersecting circles is related to  $A$  and  $B$  by:

$$\mu = \arccos (\operatorname{tg} A \operatorname{tg} B) \quad (4)$$

(see appendix)

The radiation pattern of any array antenna can be expressed by the summation of the contributions of all elements over the aperture of the array. The electric field far away from a planar array antenna in the direction (A,B) can be expressed as [5, sec 2.1]:

$$F(A,B) = \int_x \int_y E(x,y) \exp jk(x \sin A + y \sin B) dx dy \quad (5)$$

Where  $E(x,y)$  is the tangential electric field over the whole aperture and  $k = \frac{2\pi}{\lambda}$  where  $\lambda$  is the free space wavelength. An aperture distribution required for scanning in the direction  $(A_s, B_s)$  is:

$$E(x,y) = M(x,y) \exp -jk(x \sin A_s + y \sin B_s) \quad (6)$$

where  $M(x,y)$  is an amplitude taper over the aperture (real function of  $x$  and  $y$ ). Thus the electric field far away from the antenna in the direction (A,B), when a beam is formed in the direction  $(A_s, B_s)$ , is:

$$F(A,B) = \int_x \int_y M(x,y) \exp -jk\{x(\sin A - \sin A_s) + y(\sin B - \sin B_s)\} dx dy \quad (7)$$

The modulus of  $F(A,B)$  has a maximum for  $A = A_s$ ,  $B = B_s$  if  $M(x,y)$  is non-negative over the whole aperture, as is the case for a sum pattern. Any illumination  $M(x,y)$  will give rise to a broadside pattern ( $\sin A_s = \sin B_s = 0$ ) which will just be shifted over  $(\sin A_s, \sin B_s)$  when a phase factor  $\exp [-j \frac{2\pi}{\lambda}(x \sin A_s + y \sin B_s)]$  is applied. This means that any procedure to estimate echo directions for targets close to broadside can be used as well for targets in other directions.

## 6. Measuring antenna radiation patterns

In order to measure antenna patterns the complete antenna was placed in a double Cartesian suspension (see fig. 3). With this facility antenna patterns in all sections through the main beam axis can be measured by using the array antenna for transmission and measuring the field by a fixed measuring horn in the far field of the array.

The suspension system has been designed such that for any scan direction first the antenna is tilted over an angle  $\eta$  until the beam axis is horizontal and then rotated around a vertical axis (angle  $\chi$ ) in order to measure a longitudinal section of the two dimensional antenna pattern through the main beam axis. The same procedure can be used after rotation of the array around its broadside axis to get another section through the main beam axis.

Measurements of sum and difference patterns suitable for the determination of the monopulse characteristics should be made preferably along lines of constant  $\sin B$ . This would mean that the measuring horn should be vertically translated over  $r \sin B$ , where  $r$  denotes the distance from array centre to measuring horn. This however could not be accomplished at the present facility.

An approximation to the required conditions was obtained by tilting the antenna over small angles ( $\Delta\eta$ ). When the boresight axis is not horizontal a small divergence will occur between the actual section and the required  $\sin B = \text{constant}$  section.

If  $\Delta\chi$  indicates the angle over which the array is rotated around a vertical axis starting from the position in which the boresight axis lies in a vertical plane through the measuring horn and  $\Delta\eta$  is the angle in this plane between boresight axis and the horizontal line from array centre to measuring horn, the error in  $\sin B$  is:

$$\epsilon = \sin \Delta\eta (1 - \cos \Delta\chi) \quad (8)$$



(see appendix)

For the development of a monopulse algorithm antenna pattern measurements are required which are restricted to the solid angle within the 3dB contour of the main beam. For a beam in broadside this contour is a circle with a radius of 2 degrees. The beam widening during scanning requires that the solid angle to be covered has to be larger. Measurements were carried out by varying  $\Delta\chi$  continuously from  $-4^\circ$  till  $+4^\circ$  for discrete values of  $\Delta\eta$  ( $-3^\circ, -2.5^\circ, -2^\circ, \dots, +3^\circ$ ). The maximum error in the sin B co-ordinate according to (8) is 0.00013 corresponding to an angle error of  $0.007^\circ$  for a broadside beam.

Within the range of  $\Delta\eta$  and  $\Delta\chi$  mentioned (where  $\Delta\eta = \Delta\chi = 0$  indicates bore-sight or main beam axis), maps of the sum and both difference radiation patterns were recorded. This was accomplished at three radar frequencies: 5500, 5650 and 5800 MHz and for eight different scan directions:  $(A_s, B_s) = (0, 0), (0, 30), (0, 45), (30, 0), (45, 0), (30, 30), (30, 45)$  and  $(45, 30)$ .

The position of the measuring horn relative to the antenna can be adjusted by varying  $\eta$  and  $\chi$ . The corresponding phased-array co-ordinates are related to  $\eta$  and  $\chi$  by:

$$\left. \begin{aligned} \sin A &= \sin \chi \\ \sin B &= \sin \eta \cos \chi \end{aligned} \right\} \quad (9)$$

Radiation patterns as a function of  $\eta$  and  $\chi$  can be transformed to functions of  $\sin A$  and  $\sin B$  with the help of (9).

If the beam is scanned in both dimensions i.e.  $(A_s, B_s) = (30, 30), (30, 45)$  and  $(45, 30)$  a rotation of the array around the Z-axis is necessary in order to perform measurements along lines of constant  $\sin B$ . The necessary rotation  $\rho$  is given by:

$$\rho = \text{arctg} \frac{\sin A_s \sin B_s}{\cos^2 B_s} \quad (10)$$

The corresponding mechanically adjustable angles are:

$$\left. \begin{aligned} \eta &= \arctg \{ \sin (\phi-\rho) \operatorname{tg} \theta \} \\ \chi &= \arcsin \{ \cos (\phi-\rho) \sin \theta \} \end{aligned} \right\} \quad (11)$$

$$\text{where } \left. \begin{aligned} \phi &= \arctg \frac{\sin B_s}{\sin A_s} \\ \theta &= \arcsin \sqrt{\sin^2 A_s + \sin^2 B_s} \end{aligned} \right\} \quad (12)$$

are the angular co-ordinates of the boresight axis (see fig. 2). The relations (8) - (12) are derived in the appendix.

The angular estimation algorithm is based on the measurements obtained from more than 700 recorded antenna patterns. Fig. 4 shows an example of recordings of the sum and difference channels for five sections of a broadside main beam at one radar frequency. The mechanical scanning was done in the antenna's H-plane so that zero response is obtained in the  $\Delta H$  channel for  $\chi = 0$ .

The accuracy of the results depends on the accuracies of the adjusted values of  $\eta$  and of the recorded values of  $\chi$ , which are respectively 0.1 and 0.05 degree. By interchanging the E-and H-planes (by rotating the array around its broadside axis over 90 degrees) the accuracies of  $\eta$  and  $\chi$  could be checked against one another.

## 7. Results

The ratios  $\frac{\Delta E}{\Sigma}$  and  $\frac{\Delta H}{\Sigma}$ , obtained on a grid of ( $\Delta \sin A, \Delta \sin B$ ) lines, are determined for all measured points in a rectangle circumscribing the main beam's 3dB contour. Fig.5 presents an example for  $\frac{\Delta H}{\Sigma}$  with the beam scanned to  $A_s = B_s = 30^\circ$  at a frequency of 5650 MHz. From this figure it is seen that  $\frac{\Delta H}{\Sigma}$  is not completely independent of  $\Delta \sin B$  since there is a discrepancy between the values in the same column, which increases towards the edges.

This discrepancy is however small enough to warrant the simple relation

$$\Delta \sin A = f \left( \frac{\Delta H}{\Sigma} \right)$$

In the further results the dependence of  $\frac{\Delta H}{\Sigma}$  on  $\Delta \sin B$ , and  $\frac{\Delta E}{\Sigma}$  on  $\Delta \sin A$  could therefore be discarded. Fig. 6a and b show the measured quotients for all scan directions at one frequency for  $\frac{\Delta H}{\Sigma}$ - and  $\frac{\Delta E}{\Sigma}$  patterns.

The same is done in fig. 7a and b for the three frequencies combined.

In these graphs a curve is fitted through the obtained points while using a mean square error criterium. The analytical expression of these fitted curves is quite similar. This means that one single algorithm can be used to relate the difference-sum quotients with the corresponding direction sine regardless of scan direction, radar frequency and whether it concerns the  $\Delta E$  or  $\Delta H$ -channel. The resulting mean relation obtained from the fit shown in fig. 8 is

$$\text{quotient} = 2618 (\Delta \sin \chi)^3 + 21.9 (\Delta \sin \chi) \quad (13)$$

where  $\Delta \sin \chi$  is either  $\sin A - \sin A_s$  or  $\sin B - \sin B_s$ . The inverse relation obtained in a similar way via curve fitting is:

$$\Delta \sin \chi = -0.011 \text{ quotient}^3 + 0.048 \text{ quotient} \quad (14)$$

which is the relation put forward in (3).

In fig. 9a and b the maximal deviations between actual and estimated  $\sin A$  and  $\sin B$  are shown. The range of the vertical axis is from -0.1 upto 0.1 beamwidth ( $-\frac{1}{10} \sin 4^\circ$  upto  $\frac{1}{10} \sin 4^\circ$ ).

The larger spread of the results further away from the beam centre is due to the small interdependence between both difference channels.

The results for sin A estimation appear to be better than those for sin B estimation. This is due to the larger inaccuracy in adjusting and measuring the tilt angle  $\eta$  in comparison to the mechanical scan angle  $\chi$ . When the antenna is rotated over 90 degrees around its broadside axis the reverse is true: sin A estimates are inferior to sin B estimates. This indicates that part of the deviations are due to mechanical inaccuracies and that the better results are valid for both sin A and sin B estimates.

The accuracy of the estimates is better than 0.05 beamwidth within the 3dB beamwidth contour and better than 0.02 beamwidth within the contour halfway between the 3dB contour and boresight.

## 8. Conclusions

For a space-fed pencil beam phased-array antenna, equipped with suitable sum and difference channels, simple monopulse processing can provide accurate estimates of angle of arrival of target echoes.

This process contains the following steps:

- scan the beam to a direction  $(\sin A_s, \sin B_s)$  such that the target will be inside the main beam.
- determine magnitudes and relative signs of the echo signals in both difference channels and the sum channel.
- normalize the difference channel magnitudes by the sum channel magnitude  $(\frac{\Delta H}{\Sigma}$  and  $\frac{\Delta E}{\Sigma})$ .
- Compute  $\widehat{\sin A} = \sin A_s + f\left(\frac{\Delta H}{\Sigma}\right)$   
 $\widehat{\sin B} = \sin B_s + f\left(\frac{\Delta E}{\Sigma}\right)$

Where  $f$  is a polynomial of the third degree.

The indicated angle estimation procedure is simple since:

- it is independent of the scan direction (by using phased-array co-ordinates).

- the estimation algorithms for both dimensions are identical and independent.
- it is independent of the frequency over a bandwidth of more than 5 per cent.

The obtained accuracy is better than 0.05 beamwidth over the whole 3dB solid angle of the main beam and better than 0.02 beamwidth over the central quarter thereof.

#### Acknowledgment

The authors thank ir. H.J. van Schaik and F.J. Schonk for their help during measuring of the antenna patterns.

#### Literature

- [1] M.I. Skolnik: "Radar Handbook" Mc. Graw-Hill, Inc. 1970, chapter 21.
- [2] Ditto, chapter 11.
- [3] W.H. von Aulock: "Properties of Phased Arrays" Proc IRE vol. 48 p.p. 1715-1727, October 1960.
- [4] L.E. Brennan, "Angular accuracy of a phased-array radar" IRE Trans, Antennas and Propagation, vol. AP-9, p.p. 268-275, May 1961.
- [5] N. Amitay, V. Galindo, Chen Pang Wu, "Theory and Analysis of Phased Array Antennas" Wiley-Interscience, 1972.

#### Appendix

A short derivation is given of the relations quoted in the paper. A number of them is known from literature. For consistency they are included.

Spherical co-ordinates  $(\theta, \phi)$  or phased-array co-ordinates  $(\sin A, \sin B)$  can be used to indicate any direction relative to the array's Cartesian co-ordinate system  $(X, Y, Z)$ , where X is the central antenna row, Y the central

antenna column, and Z the broadside direction. Assume a unit sphere around the array centre O. As can be seen in fig. 10 the following relations hold when P is any point on the unit sphere.

$$PP_x = \sin A = SP_y = OQ$$

$$PP_y = \sin B = SP_x = OR$$

$$\theta = \arcsin \frac{PS}{OP} = \arcsin OP_z = \arcsin \sqrt{OQ^2 + OR^2}$$

$$= \arcsin \sqrt{\sin^2 A + \sin^2 B}$$

$$\phi = \arctg \frac{QP_z}{OQ} = \arctg \frac{\sin B}{\sin A}$$

(11)

Tilt ( $\eta$ ) and rotation of the antenna around the vertical ( $\chi$ ), which are used to position the beam axis towards the measuring horn, can be interpreted as a corresponding movement of the horn relative to a stationary antenna.

If the horn is positioned in direction P its tilt and rotation are:

$$\eta = \angle P_x OS$$

$$\chi = \angle P_x OP = A$$

$$\text{So } P_x S = \sin B = P_x O \sin \eta = \cos A \sin \eta$$

and thus

$$\sin A = \sin \chi$$

$$\sin B = \sin \eta \cos \chi$$

(9)

$\eta$  and  $\chi$  can be expressed in terms of the polar co-ordinates of the measuring horn:

$$\eta = \arctg \frac{P_x S}{S O}$$

Where  $SO = \cos \theta$

$$P_x S = PP_y = P_z Q = OP_z \sin \phi = SP \sin \phi = \sin \theta \sin \phi$$

thus

$$\left. \begin{aligned} \eta &= \text{arctg} (\sin \phi \text{tg } \theta) \\ \chi &= \text{arc sin } \frac{PP_x}{OP} = \text{arcsin } RP_z = \text{arcsin } (OP_z \cos \phi) \\ &= \text{arsin } (\cos \phi \sin \theta) \end{aligned} \right\} (10)$$

If the antenna is rotated around the Z-axis over an angle  $\rho$ , which is done in order to keep B constant while  $\chi$  is varied with  $\eta$  fixed, this will change  $\phi$  into  $\phi - \rho$ .

So

$$\left. \begin{aligned} \eta &= \text{arctg} \{ \sin (\phi - \rho) \text{tg } \theta \} \\ \chi &= \text{arcsin } \{ \cos (\phi - \rho) \sin \theta \} \end{aligned} \right\} (11)$$

The angle  $\mu$  between intersecting lines of constant  $\sin A$  and  $\sin B$  on the unit sphere can be derived from fig. 11.

The point P has angular co-ordinates A and B. The corresponding circles intersect under an angle  $\mu$ . The plane which is tangential to the sphere in P intersects the X-Y-Z-axes at distances  $\frac{1}{\sin A}$ ,  $\frac{1}{\sin B}$  and  $\frac{1}{\sqrt{1-\sin^2 A - \sin^2 B}}$  from the origin.  $\Delta SOT$  is rectangular so:

$$ST = \sqrt{\frac{1}{1-\sin^2 A - \sin^2 B} + \frac{1}{\sin^2 B}}$$

$\Delta SOQ$  is rectangular with  $\angle OSQ = B$  and  $OS = \frac{1}{\sin B}$  so  $OQ = \frac{1}{\cos B}$

$$\Delta T O Q \text{ is rectangular with } T O = \frac{1}{\sqrt{1 - \sin^2 A - \sin^2 B}}$$

$$\text{so } T Q = \sqrt{\frac{1}{1 - \sin^2 A - \sin^2 B} - \frac{1}{\cos^2 B}}$$

$\Delta S T Q$  is rectangular with  $\angle S T Q = \mu$  so

$$\mu = \arccos \frac{T Q}{T S} = \arccos (\operatorname{tg} A \operatorname{tg} B) \quad (4)$$

When the beam is scanned in both dimensions, the direction in which mechanical scanning takes place during measurements is not parallel to lines of constant  $\sin B$ . In order to remedy this the antenna is rotated over an angle  $\rho$  around the Z-axis as shown in fig. 12.

As before:

$$\begin{aligned} R P_z &= \sin A \\ P P_z &= \sqrt{1 - \sin^2 A - \sin^2 B} \\ O R &= \sin B \\ \text{and } R P &= \cos B \end{aligned}$$

$\Delta R P P_z$  is similar to  $\Delta P U P_z$  so

$$U P_z = P P_z \frac{P P_z}{R P_z} = \frac{1 - \sin^2 A - \sin^2 B}{\sin A} \quad \text{and}$$

$$U R = R P_z + U P_z = \frac{\cos^2 B}{\sin A}$$

The required rotation is equal to  $\angle R U O$  so:

$$\rho = \operatorname{arctg} \frac{O R}{U R} = \operatorname{arctg} \frac{\sin A \sin B}{\cos^2 B} \quad (10)$$



When a broadside beam pattern is to be measured the measuring horn is placed along the broadside axis of the array, i.e. the Z-axis. Then several sections through the beam patterns are obtained by varying the mechanical scan angle  $\chi$  for several values of the tilt angle  $\eta$ . The corresponding paths in sine space, which are the projections of the moving point P in fig.13, are not lines with constant  $\sin B$  but are ellipses.

$$\angle OP_1Q = \chi \text{ so } QP_1 = \cos \chi$$

$$\angle P_{1z}P_1Q = \eta \text{ so } P_{1z}Q = \sin \eta \cos \chi$$

$$P_zO = \sin \eta$$

Instead of the required value of  $\sin B = \sin \eta$  the recorded value is  $\sin \eta \cos \chi$ .

The corresponding error is:

$$\epsilon = \sin \eta (1 - \cos \chi)$$

For scanned beam positions the same situation exists relative to boresight.

The corresponding error in  $\Delta \sin B$  is:

$$\epsilon = \sin \Delta \eta (1 - \cos \Delta \chi) \quad (8)$$

Ferdinand B. Rijsdijk was born in Rotterdam, The Netherlands, on October 24, 1949. He received the M.S. degree in electrical engineering from the University of Technology, Delft, in 1974. From 1974 until 1976 he worked at the Physics Laboratory of the Organization for Applied Scientific Research in the Netherlands TNO on an experimental phased-array radar system.

Gerard A. van der Spek (M'68) was born in Leiden, The Netherlands, on October 7, 1935. He received the M.S. degree in electrical engineering from the University of Technology, Delft, in 1961. In 1960 he joined the Physics Laboratory TNO, where he has been working on problems of digital data transmission, statistical detection theory and signal processing. Presently he is involved in the design of an experimental phased-array radar system.

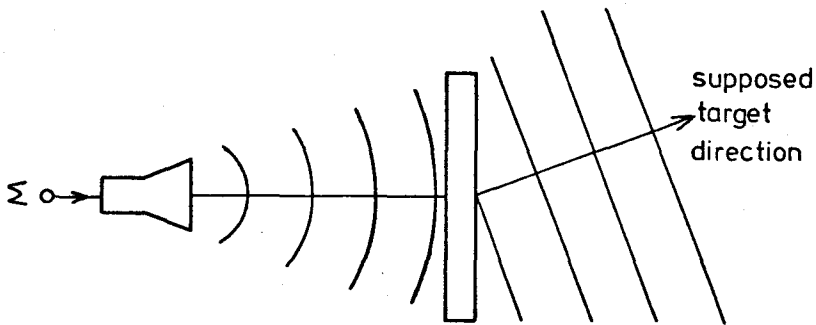


Fig 1a: Transmission towards a target. (seen from above)

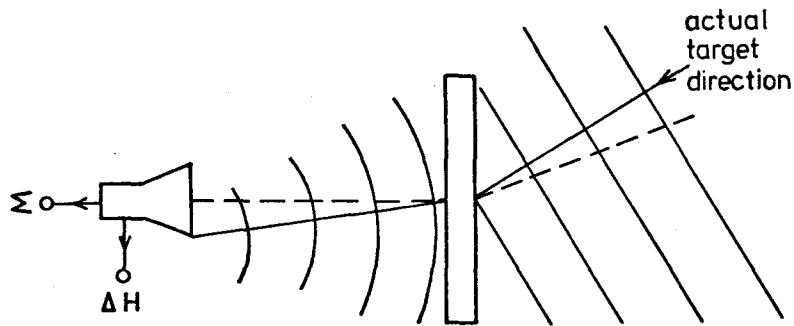


Fig 1b: Reception from a target.

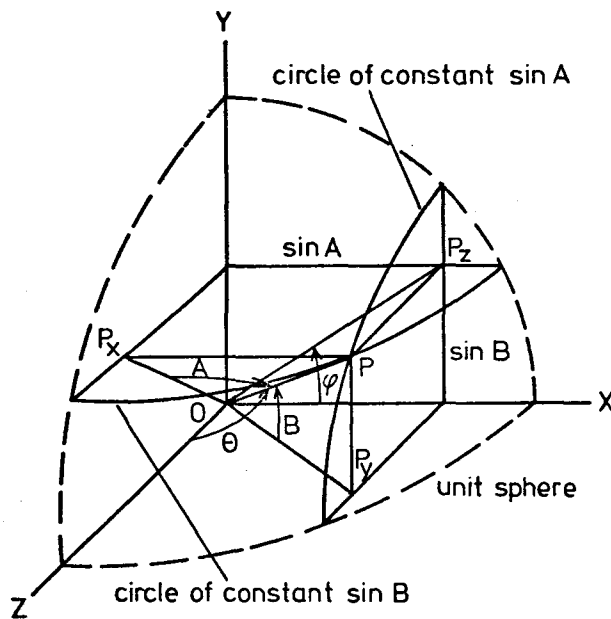


Fig. 2: Relation between rectangular Cartesian-, spherical- and phased-array co-ordinate systems.

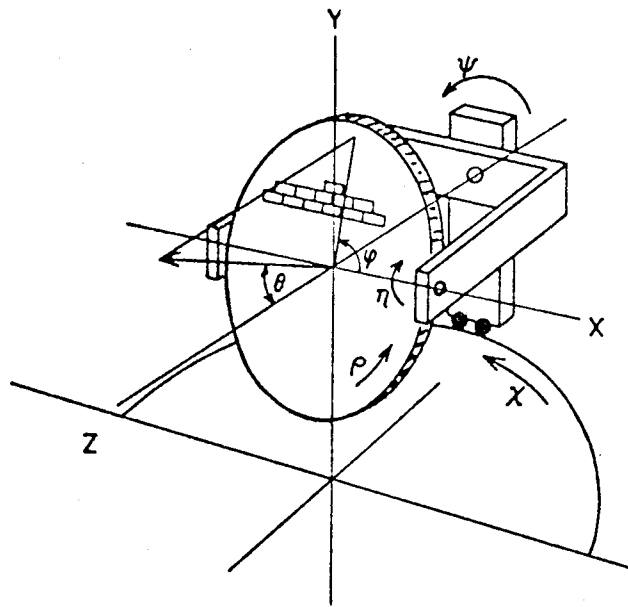


Fig. 3: Double Cartesian Suspension system.

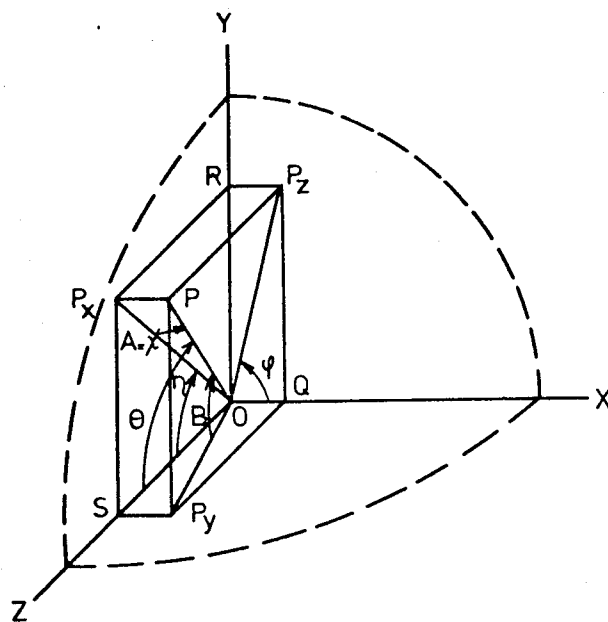


Fig. 10: Relation between  $(A,B)$ ,  $(\theta;\phi)$  and  $(X,n)$ .

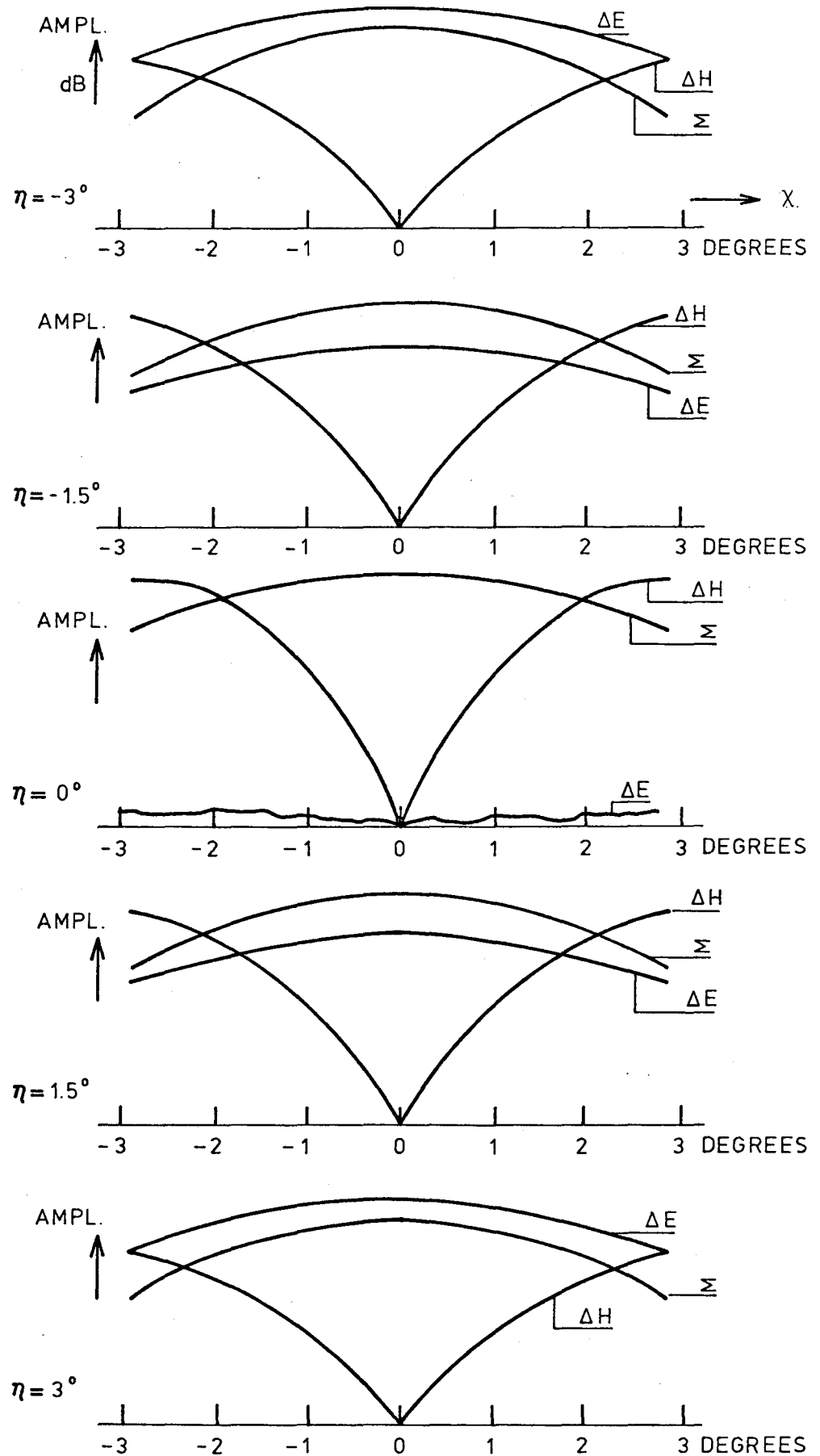


Fig. 4: Example of measured sum and difference antenna patterns. Logarithm of modulus of channel output vs. mechanical scan angle for 5 tilt values.

$\Delta \sin B$ x 100	$\frac{\Delta H}{\Sigma}$												
-3.38	-1.27	-.98	-.73	-.52	-.33	-.16	.00	.16	.32	.49	.68	.88	1.11
-2.78	-1.22	-.97	-.72	-.51	-.32	-.16	.00	.16	.31	.48	.68	.87	1.08
-2.18	-1.17	-.93	-.71	-.51	-.32	-.15	.00	.15	.32	.48	.67	.86	1.07
-1.58	-1.15	-.91	-.69	-.50	-.31	-.15	.00	.15	.31	.47	.65	.84	1.04
-.99	-1.12	-.89	-.69	-.50	-.32	-.15	.00	.15	.31	.48	.66	.85	1.06
-.39	-1.08	-.87	-.66	-.48	-.31	-.15	.00	.15	.30	.45	.63	.83	1.01
.20	-1.10	-.89	-.66	-.49	-.31	-.15	.00	.15	.31	.47	.65	.83	1.04
.78	-1.11	-.88	-.68	-.48	-.31	-.15	.00	.15	.30	.47	.64	.83	1.02
1.37	-1.14	-.88	-.68	-.49	-.32	-.15	.00	.15	.31	.46	.64	.83	1.05
1.95	-1.12	-.89	-.68	-.49	-.31	-.15	.00	.15	.31	.47	.65	.85	1.07
2.53	-1.16	-.91	-.68	-.50	-.32	-.15	.00	.16	.32	.48	.66	.87	1.11
3.11	-1.19	-.92	-.69	-.50	-.32	-.16	.00	.16	.32	.48	.66	.87	1.10
3.68	-1.23	-.94	-.71	-.51	-.33	-.17	.00	.17	.32	.50	.69	.91	1.15
$\Delta \sin A$ x 100	-4.36	-3.62	-2.89	-2.16	-1.44	-.72	0.00	.71	1.41	2.11	2.81	3.50	4.16

fig. 5:  $\frac{\Delta H}{\Sigma}$  as a function of  $\Delta \sin A$  for different  $\Delta \sin B$  values.

Scan direction  $A_s = B_s = 30^\circ$

--- rectangle circumscribing 3 dB-contour

ALL H DIFFERENCE PATTERNS  
QUOTIENT=F(SINA)  
FOR DIFFERENT SINB

FREQ=5650 MHZ  
ALL MEASURED SCANDIRECTIONS

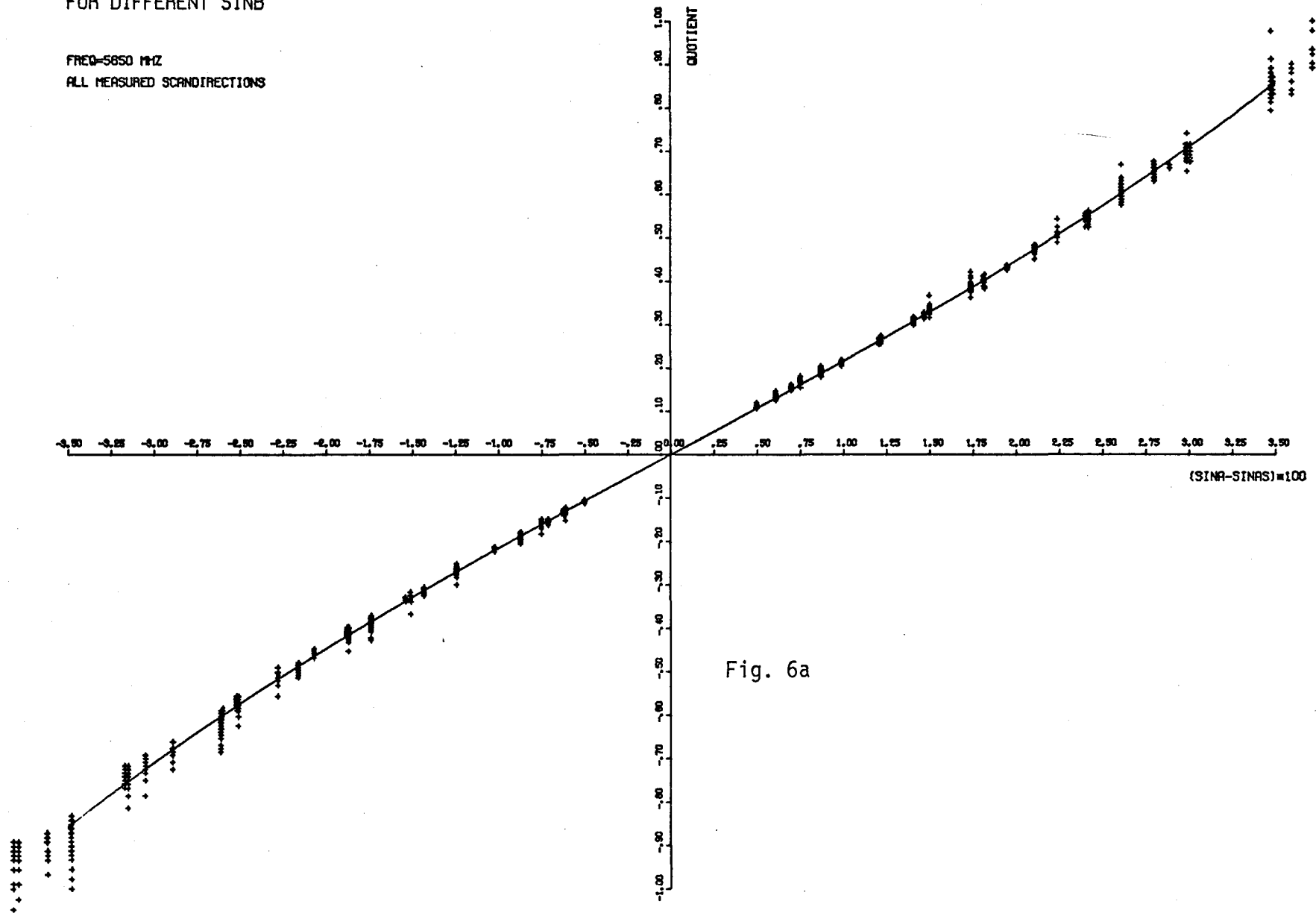


Fig. 6a

ALL E DIFFERENCE PATTERNS  
QUOTIENT=F(SINB)  
FOR DIFFERENT SIN A

FREQ=5650 MHZ  
ALL MEASURED SCANDIRECTIONS

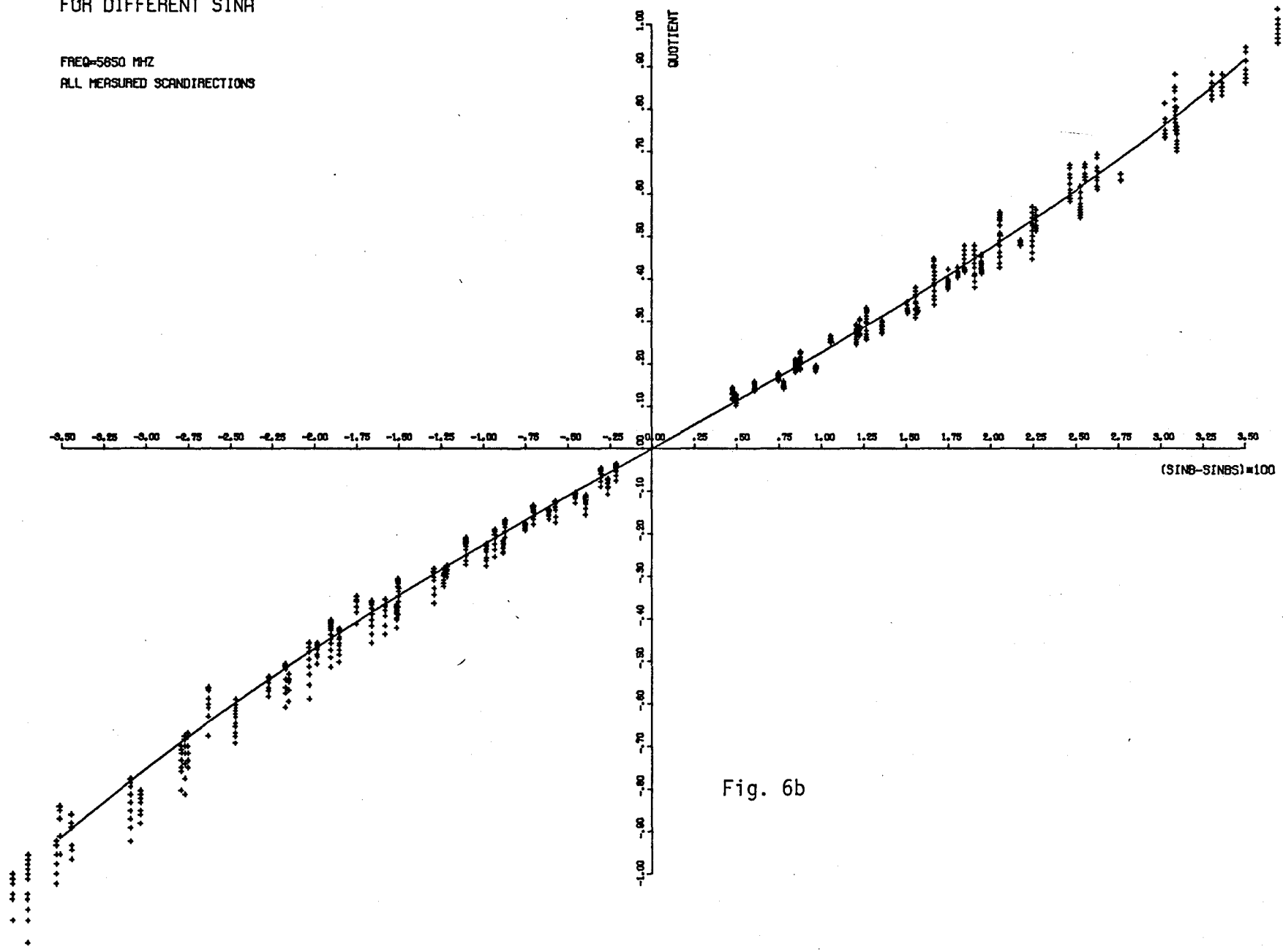


Fig. 6b



ALL H DIFFERENCE PATTERNS  
QUOTIENT=F(SINA)  
FOR DIFFERENT SINB

ALL MEASURED FREQUENCIES  
ALL MEASURED SCANDIRECTIONS

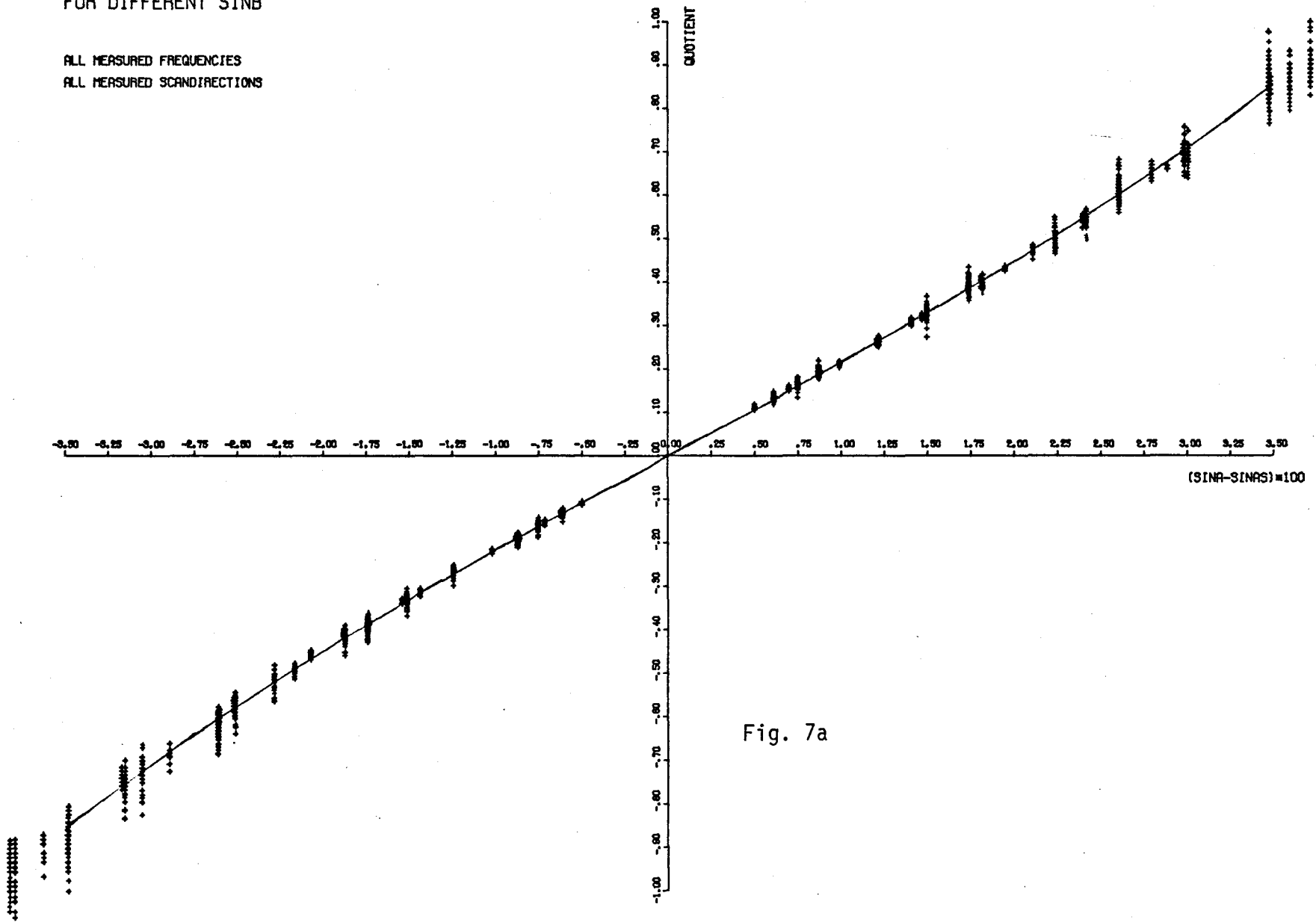


Fig. 7a

ALL E DIFFERENCE PATTERNS  
QUOTIENT=F(SINB)  
FOR DIFFERENT SIN A

ALL MEASURED FREQUENCIES  
ALL MEASURED SCANDIRECTIONS

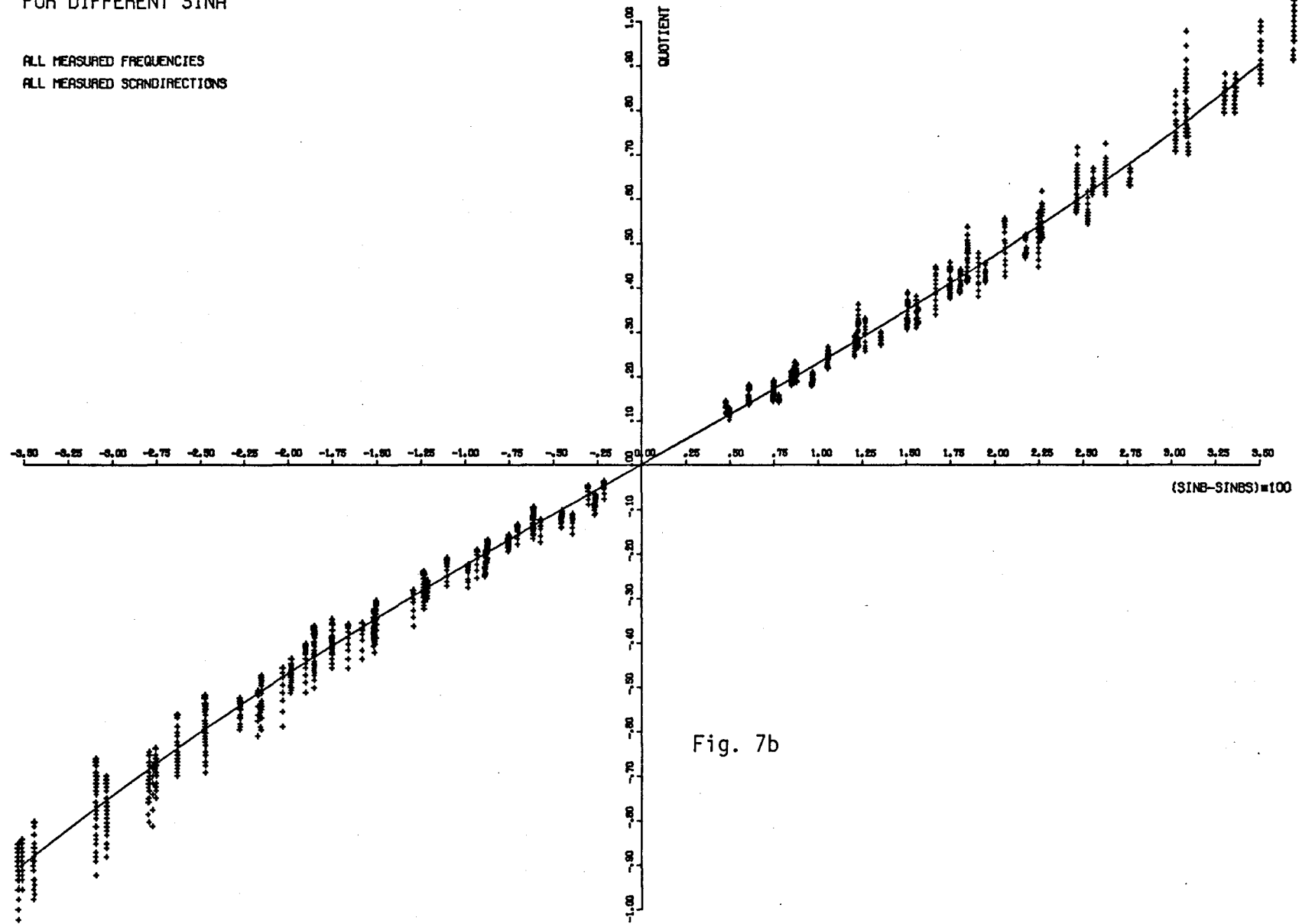


Fig. 7b

ALL DIFFERENCE PATTERNS  
QUOTIENT=F(SIN-)

ALL MEASURED FREQUENCIES  
ALL MEASURED SCANDIRECTIONS

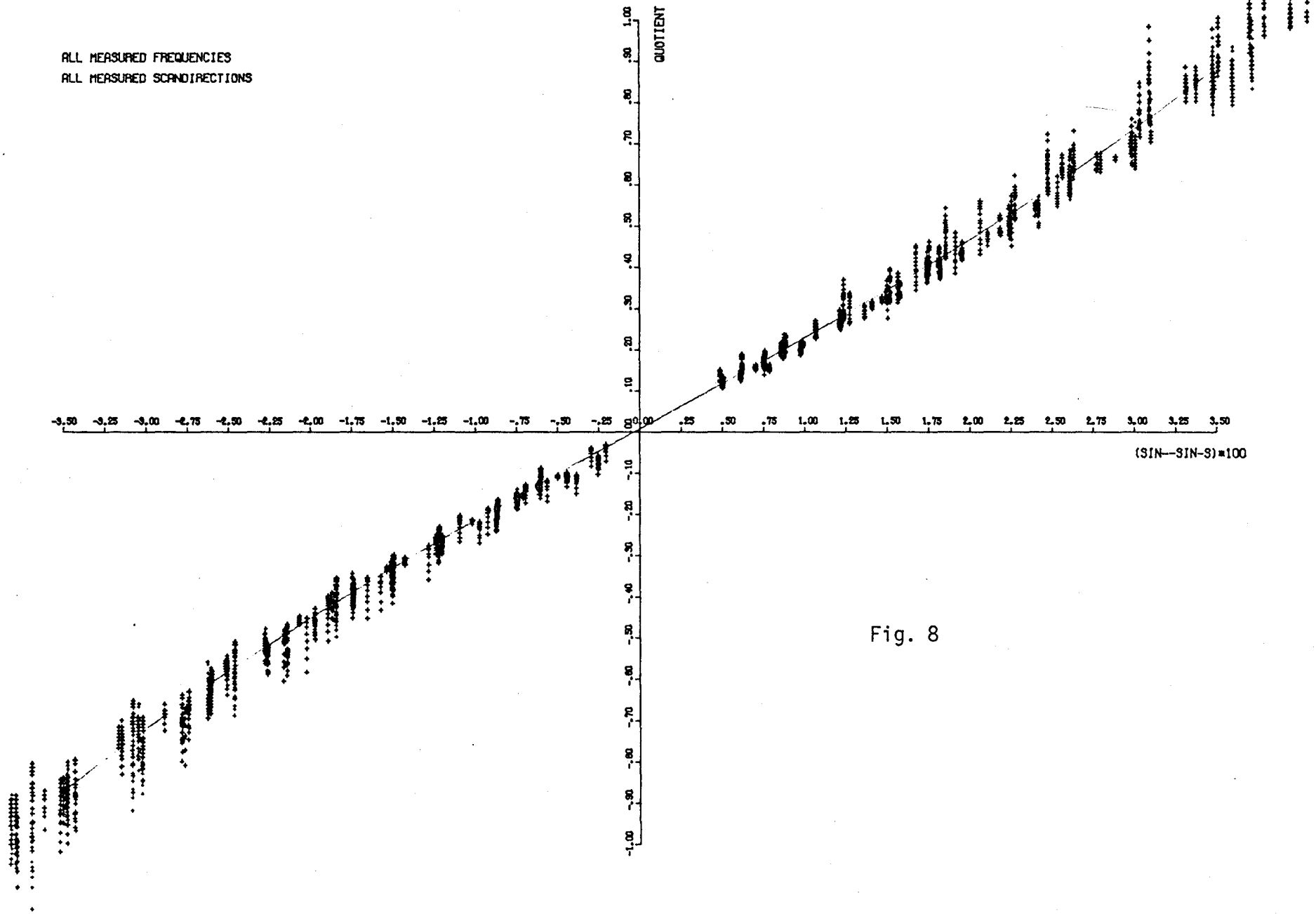


Fig. 8

ALL H DIFFERENCE PATTERNS  
MAX. DEVIATION=F(SINA)

ALL MEASURED FREQUENCIES  
ALL MEASURED SCANDIRECTIONS

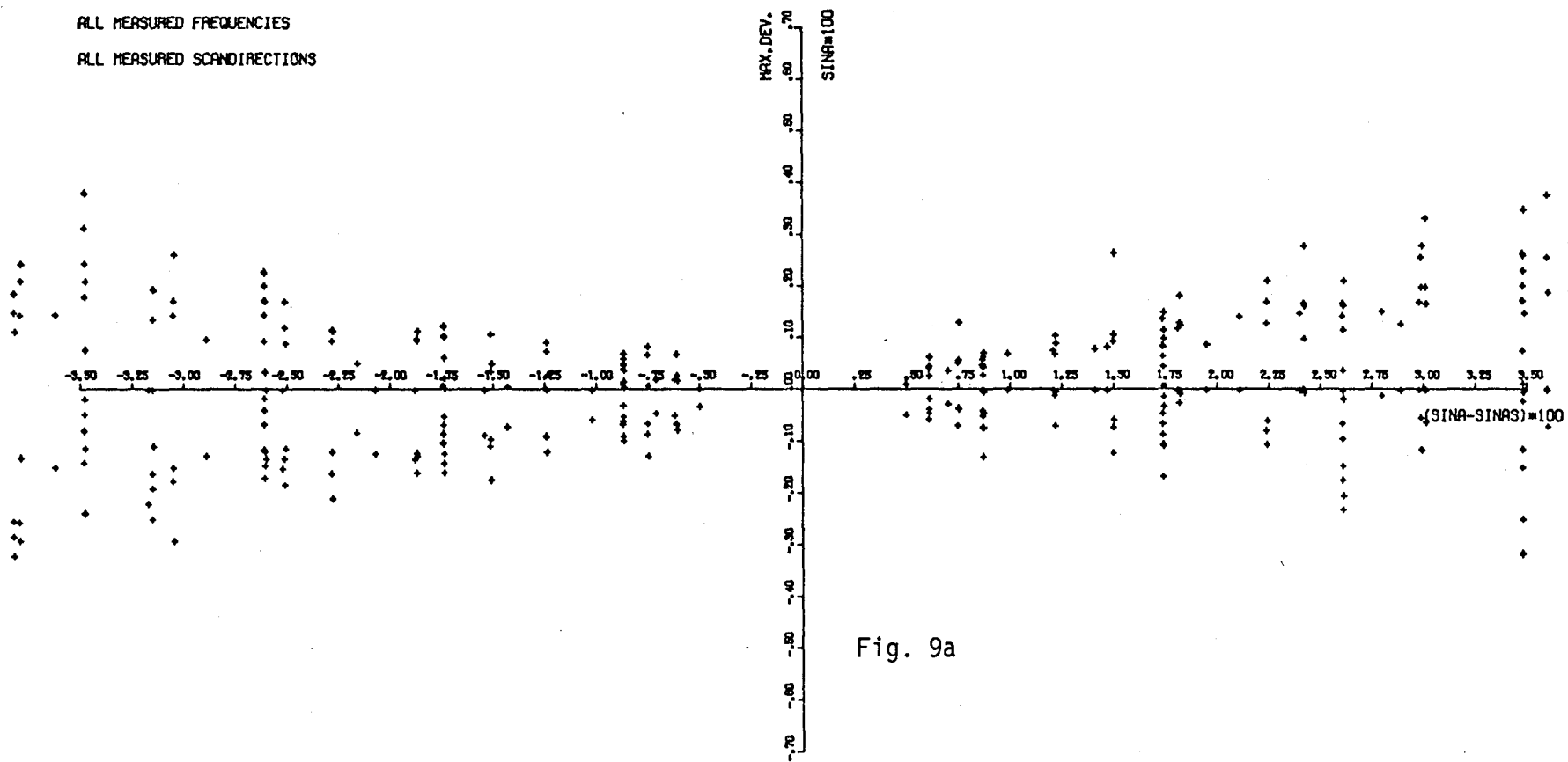


Fig. 9a

ALL E DIFFERENCE PATTERNS  
MAX. DEVIATION=F(SINB)

ALL MEASURED FREQUENCIES  
ALL MEASURED SCANDIRECTIONS

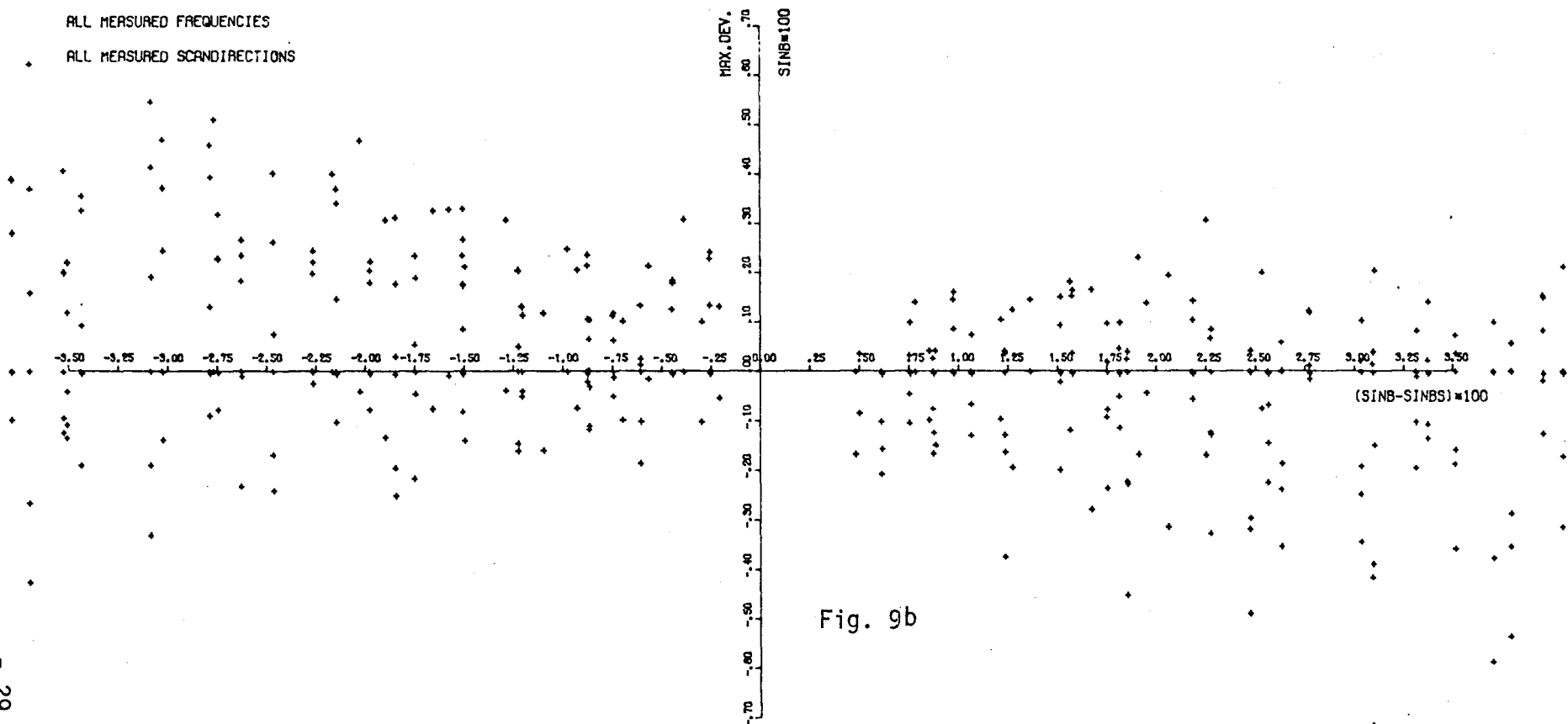


Fig. 9b



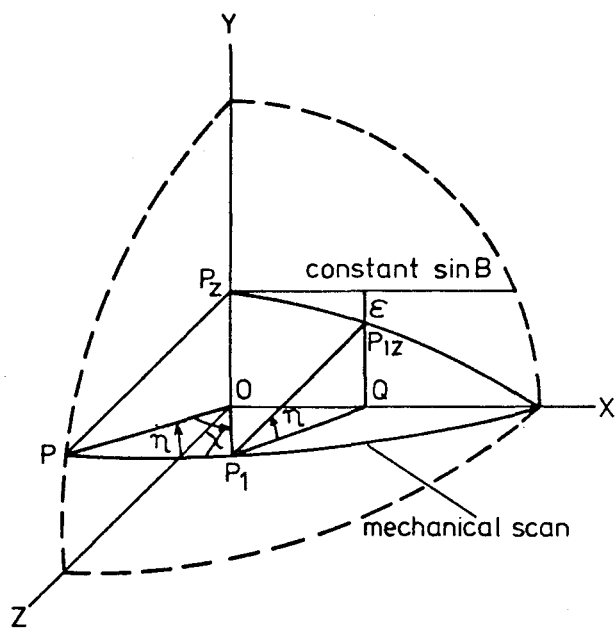


Fig. 13: Error in sin B - grid when measuring a broadside beam pattern.